Available online at sjuoz.uoz.edu.krd

Science Journal of University of Zakho

Vol. 5, No.1, pp. 79 –87, March-2017

p-ISSN: 2410-7549
e-ISSN: 2414-6943

SYNTHESIS AND CHARACTERIZATION OF PHOTOCATALYTIC PERFORMANCE OF RUTILE-TIO$_2$ NANOROD ARRAYS FOR SOLAR HYDROGEN GENERATION

Amin K.Qasim1[a,*], Lazgin A.Jamil [a], Qiao chen [b]

[a] Dept. of Chemistry, Faculty of Science, University of Zakho, Zakho, Kurdistan Region, Iraq - (amin.qasim, lazgin.jamil)@uoz.edu.krd

[b] Dept. of Chemistry, School of Life Sciences, University of Sussex, Brighton, BN1 9QJ, UK.

Received: Nov. 2016 / Accepted: Mar. 2017 / Published: Mar. 2017

ABSTRACT:
Single crystalline rutile TiO_2 nanorods (TNRs) films have been grown on the fluorine doped tin oxide (FTO) substrates using a one pot hydrothermal method, have attracted great attention because of favorable applications in the photoelectrochemical water splitting system. The effect of the reaction conditions on the morphology, crystal orientation and photocatalytic activity has been systematically investigated. The X-ray diffraction (XRD) pattern shows that two diffraction peaks at 36.3° and 63.2° correspond to the (101) and (002) planes of the tetragonal rutile TiO_2 nanorod, respectively. The scanning electron microscope (SEM) of the samples indicates that the TiO_2 array surface morphology and orientation are highly dependent on the reaction parameters, such as temperature, reaction time and the titanium precursor concentration. In a typical condition of the hydrothermal method at 0.3ml of TBO and 160°C for 3 hr, a small diameter and short length 190 nm and 2.2 µm of TiO_2 nanorods respectively, are grown on florien doped tin oxide (FTO) substrate. When synthesized TiO_2 nanorods photocatalyst was irradiated under illumination of simulated AM 1.5G solar light (100 mW cm^{-2}) achieves an overall Photocurrent density of 1.80 mA/cm^2 with a maximum photoconversion efficiency of ~1.6%. The results suggest that these dense and aligned one-dimensional TiO_2 nanorods are promising for hydrogen generation from water splitting based on PEC cells.

KEYWORDS: Photocatalytic, Rutial-TiO_2 Nanorod, Solar Hydrogen Generation, Hydrothermal Synthesis.

1. INTRODUCTION

Hydrogen is considered as an ideal fuel for the future due to, it is cleaning, energy efficient, and abundant in nature, also hydrogen fuel can be produced from clean and renewable energy sources and, thus, its life cycle is clean and renewable. Solar and wind are the two major sources of renewable energy and they are also the promising sources for renewable hydrogen production. However, presently, renewable energy contributes only about 5% of the commercial hydrogen production primarily via water electrolysis, while other 95% hydrogen is mainly derived from fossil fuels (Meng et al., 2004).

Since Fujishima and Honda discovered the Photocatalytic activity of TiO_2 in water splitting, a large amount of studies have focused on TiO_2 based photo-catalysts (Fujishima, 1972; Hashimoto et al., 2005). As one of the most multi-functional materials, nanocrystalline TiO_2 are always of interest to material scientist for its excellent properties, such as good photocatalysis, high photoelectricity conversion efficiency, high photo-refractive index, super-stability in chemical reactions, and good biological compatibility. As a result, it has found applications in many areas such as including the decomposition of toxic pollutants, photocatalytic water splitting, gas sensors, biosensors, quantum dot solar cells, chemical stability in severe environments, and superior Photocatalytic properties (Guldin et al., 2013; Liu et al., 2013; Lou et al., 2013; Pan et al., 2001; Wu et al., 2011).The electrical, optical, and chemical reactions on the surface of these materials determine the performance of their devices.

Titanium oxide (TiO_2) is a non-toxic, chemically and mechanically stable semiconductor material. TiO_2 is an important semiconductor material for use in a wide range of applications, including photocatalysis, environmental pollution control and solar energy conversion (Selman and Hassan 2015;Shen et al., 2008; Tsai and Teng, 2006). It is well known that TiO_2 exists in three crystalline polymorphs, namely, rutile (tetragonal), anatase (tetragonal) and brookite (orthorhombic). Rutile is the most stable phase, whereas anatase and brookite are metastable phase and transform to rutile upon heating.(Hosono et al., 2004; Kolen'ko et al., 2003).

The rutile phase has been widely used as pigment materials or as colouring agent because of its chemical stability. However, the anatase phase has been widely used in photodegradation due to its photochemical stability and high photoactivity.(Fujishima et al., 2000; Selman and Hassan, 2015; Shen et al., 2008).

Quasi-one-dimensional (1D) nanostructures (nanorod, nanowire, nanofibre, nanotube etc.) are of both theoretical and technological interest for their novel properties in use as electronic and optoelectronic devices, resonators and cantilevers, chemical sensors and so on, showing promising application in almost all high technology areas (Dai, 2002; Kazes et al., 2002; Peng et al., 2000; Wang and Song, 2006).

TiO_2 nanorod arrays, which are considered to be one of the significant n-type semiconductor materials, provide uninterrupted electrical pathways for photogenerated electrons compared with several other morphological TiO_2 anodes for PEC water splitting such as TiO_2 polycrystalline or mesoporous films (Char et al., 2008; Lin et al., 2012).

TiO_2 nanowire/nanorods have been synthesized using several methods, such as chemical vapour deposition (CVD), (Lee et al.,2007) physical vapour deposition (PVD), (Wolcott et al., 2009) vapour-liquid-solid growth (VLS), (Lee et al., 2006) and

* Corresponding author

template sol-gel method, (Lei et al., 2001) mostly, hydrothermal reaction with an assistance of surfactant and copolymer. Recently, single crystalline TiO_2 nanorods with a rutile phase have been successfully grown on the top of fluorine-doped tin oxide (FTO) films coated glass, by a hydrothermal method. Since the single crystalline rutile nanorods grown by this method are in a direct contact with the FTO film, no complicated procedure is needed to form the bottom electrode for subsequent device fabrication.(Feng et al., 2008; Liu and Aydil, 2009).

Hydrothermal methods are the preferred procedure for synthesizing large quantities of TNRs with high reproducibility and low cost. However, there is still a challenge in terms of optimizing the electrical and photocatalytic properties of these nanostructures. Although previous works have been focused on known applications and performance comparisons, there is a lack of knowledge concerning several aspects related to the effect of the sample synthesis conditions on its final performance in PEC application. (Kim and Yang, 2015)

When specifically compared to other methods, the hydrothermal method has several advantages. First, a single- and poly-crystalline product can be directly obtained at a relatively lower reaction temperature (in general <250 C°) without a sintering process, resulting in a transformation from the amorphous phase to the crystal phase. Second, by changing the hydrothermal conditions (such as temperature, pH, reactant concentration and molar ratio, and additives), crystalline products could be easily modified with different compositions, structures, and morphologies. Third, the required equipment and processing conditions are simpler than sol-gel method and controlling the reaction conditions is easier. Therefore, the hydrothermal method is attractive for preparing transition metal oxides as a photocatalyst. (Sun et al., 2013; Xie et al., 2013; Zou et al., 2012).

In this study, we report a new, simple and rapid synthetic route to produce rutile TiO_2 nanorods and influence of the hydrothermal synthesis conditions on the photocatalytic activity of the rutile TiO_2 nanorods as photo-anode materials for PEC water splitting; the conditions studied included the titanium source concentration, growth temperature and growth time.

2. EXPERIMENTAL DETAILS

2.1 Preparation of TiO_2 Nanorod Array

All the chemicals used throughout this project were analytical grade and used as received. Hydrochloric acid (Fisher Scientific, 32 wt. %, d= 1.16), titanium (IV) n-butoxide (Alfa Aesar, 99+ %) and Florien doped tin oxide (FTO) coated glass (Sigma Aldrich, D= 2mm, 7Ω/sq.) was used as the substrate. TiO_2 nanorod (NR) films were grown on a substrate of fluorine doped tin oxide (FTO) glass. Prior to the synthesis, the fluorine doped tin oxide /glass substrates (1 x 2 cm^2) were sonicated in a solution of methanol, propanone and deionized (DI) water (1: 1: 1 volume ratio) for 20 minutes and rinsed with DI water for several times, followed by drying in air.

TiO_2 nanorod films were synthesized by using a hydrothermal method in a 50 ml Teflon lined stainless steel autoclave. To ensure the temperature and pressure for each reaction was consistent, the samples were heated in a gas chromatography (GC, Perkin Elmer auto system). In a typical synthesis, hydrochloric acid (14 ml of 32% HCl by Wt. %) was added to DI water (10 ml) and magnetically stirred for 5 minutes, after which, titanium butoxide (TBO, Alfa Aesar, 0.3 - 0.6 ml) was added to the reaction solution and magnetically stirred for a further 5 minutes. The reaction solution was transferred to the autoclave, containing a piece of FTO glass (1 x 2 cm^2), where the conductive side is facing down. The autoclave was sealed and placed in the GC oven (preheated to 150 - 180 °C) for 2 - 16 hours, after this reaction, the sample was removed from the autoclave thoroughly washed with deionized water and dried. To improve the crystallinity of the nanorod film and its adhesion to the substrate subsequently annealed in air at 550 °C for 3 hours.

2.2 Structure Characterisations

The morphology observation of bare FTO substrates and TiO_2 nanorod grown on FTO substrates was operated by a scanning electron microscope (SEM) (JSM 820M, Jeol). The average diameters and average film thicknesses were measured from top- and side-view SEM images using Image J (National Institutes of Health, USA). The crystallinity and structure orientation of the nanostructures were analyzed by powder XRD (Siemens D500), all the samples were measured in the continuous scan mode in the 2θ range of 20-70°, using a scan rate of 0.02 deg/s. The Photo -electrochemical performance of the nanorod array photoanode was measured with a three-electrode cell with a Pt wire as the counter electrode and Ag/AgCl as the reference electrode and TiO_2 samples were used as a working electrode. An aqueous solution containing 1M KOH (with measured pH of 13.2) was used as the electrolyte. The electrochemical potential and current were controlled by a USB potentiostat (eDAQ EA163). In order to simulate sunlight, a 300 W xenon lamp with AM 1.5 filters was used as the light source. The power intensity of the light was adjusted to 100 $mWcm^{-2}$.

3. RESULTS AND DISCUSSION

3.1 Controlling the Growth Parameters for Optimising the TiO_2 NRs Film

3.1.1 Effect of Initial Titanium Concentration: During the examination of the influence of initial TBO precursor concentration, all other parameters such as growth time and temperature were maintained constant three hours and at150°C respectively. The initial TBO volumes used were 0.3, 0.4 and 0.5 ml; this corresponds to 1.23, 1.63 and 2.04 % of the total reaction solution, with all other concentrations a homogenous white film covered the FTO substrate. When 0.3 ml TBO was used as the initial volume, as shown in Fig.1, both width and length of the nanorods increase with increasing TBO concentration. It also can be seen that from Fig.1, increasing the initial TBO volume causes an increase in the film and improvement of the orientation of the rods along the c-axis. Increasing the TBO volume of 0.4 ml, TNRs had almost doubled in average width at 350 nm, and length 2.8 µm and had started to merge with neighbouring NRs. At 0.5 ml TBO, the TNRs had mostly combined together, resulting in a breakdown of nanostructure, so at high concentrations, when the nucleation density is high, the growth of the angled rods is hindered by neighbouring rods that are more aligned to the substrate surface.

The diameter distribution of the nanorods is plotted in Figure 2 (A). The average size and diameter of the NRs were evaluated from (100 measurements) through their top view SEM images. It is noted that the diameter and the length of the nanorods increase with increasing the TBO concentration. When 0.3 ml of the TBO added as initial volume, average width at 180 nm, and length 1.9 µm, by increasing the volume of the titanium source to 0.4 ml, the average rod diameter of 350 nm and film thickness of 2.8 µm, which indicates a greater variation in rod diameter. It was also observed that using higher titanium butoxide concentrations led to poor film adheres to the substrate. In addition, the crystal domain of TNRs can be calculated via Debye–Scherrer equation. (Waterhouse and Waterland, 2007).

$$D = \frac{K\lambda}{\beta \cos\theta} \qquad (1)$$

Where D is the crystalline diameter, K is the shape factor (0.89 in this work), λ is the wavelength of the X-ray source (Cu target, λ = 1.541 Å), θ is the Bragg angle of the diffraction peak (in degrees) and β is the linewidth of the diffraction peak corrected for instrument broadening (in radians).

From the diffraction spectrum shown in Figure 3 of three different volumes 0.3, 0.4 and 0.5ml of TBO, the (002) peak is the narrowest peak with a FWHM of 0.7°, 0.6° and 0.59°, which corresponds to a crystal domain size of 11.45, 13.43 and 13.57 nm respectively, this suggests that the large crystal domain with less defects is essential for high charge mobility with less probability of charge recombination. Therefore, variation of FWHM with different volumes indicates a greater variation in rod diameter.

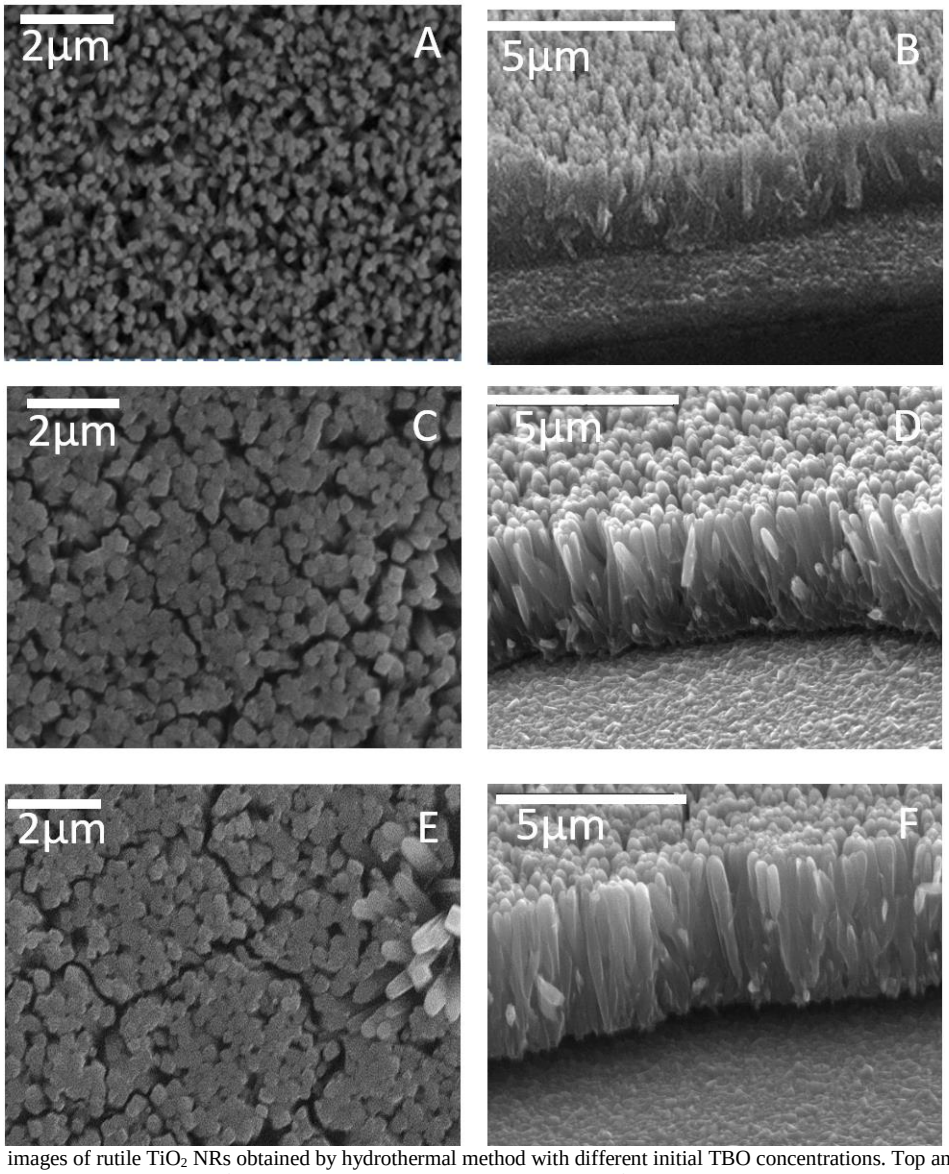

Figure 1. SEM images of rutile TiO_2 NRs obtained by hydrothermal method with different initial TBO concentrations. Top and cross section view of: (A, B) 0.3 ml, (C, D) 0.4 ml, (E, F) 0.5 ml of TBO respectively

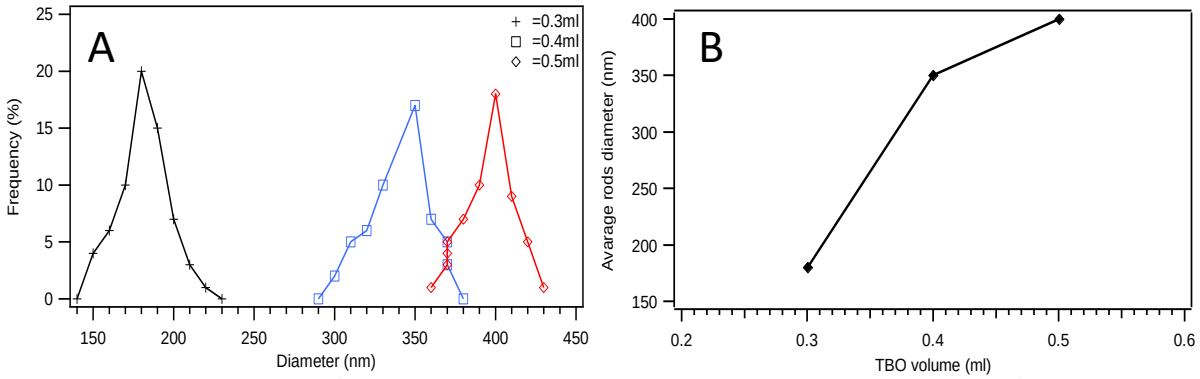

Figure 2. (A) Diameter distribution of TiO_2 nanorod arrays prepared on an FTO substrate with varied TBO volume of 0.3ml, 0.4ml, and 0.5ml. (B): Average rod diameter as function to the titanium precursor volume.

Figure 3, shows the XRD pattern of the TiO_2 nanorods grown on FTO/glass substrates. The crystal structure and crystal orientation of the as grown TNRs were investigated by powder XRD. And XRD patterns of TiO_2 nanorods films prepared using different initial titanium volumes were collected and are presented in Fig. 3, all samples were annealed in air for three hours at 550 °C to increases the crystallinity of the structure and also the adhesion of the TiO_2 film to the substrate. Two diffraction peaks at 36.3° and 63.2° correspond to the (101) and (002) planes of the tetragonal rutile TiO_2 crystal structure, respectively, are analysed based on the Joint Committee on Powder Diffraction Standards database (JCPDS No. 88-1175) (Thamaphat et al., 2008), which indicates that the highly oriented rutile layer was formed on the FTO film. The relationship between these two peaks were investigated, with a volume of 0.4 ml TBO forming tilted TNRs, giving a dominant peak of (101). As the volume of TBO increases from 0.5 ml to 0.6 ml, the NR orientation becomes closer to the surface normal, decreasing the (101) and increasing the (002) peak as shown in Figure 3.

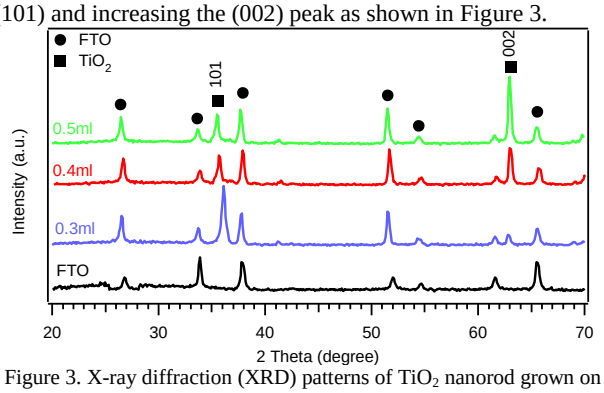

Figure 3. X-ray diffraction (XRD) patterns of TiO_2 nanorod grown on FTO substrates. These films were created using three different titanium butoxide (TBO) volumes and annealed at 550°C for three hours.

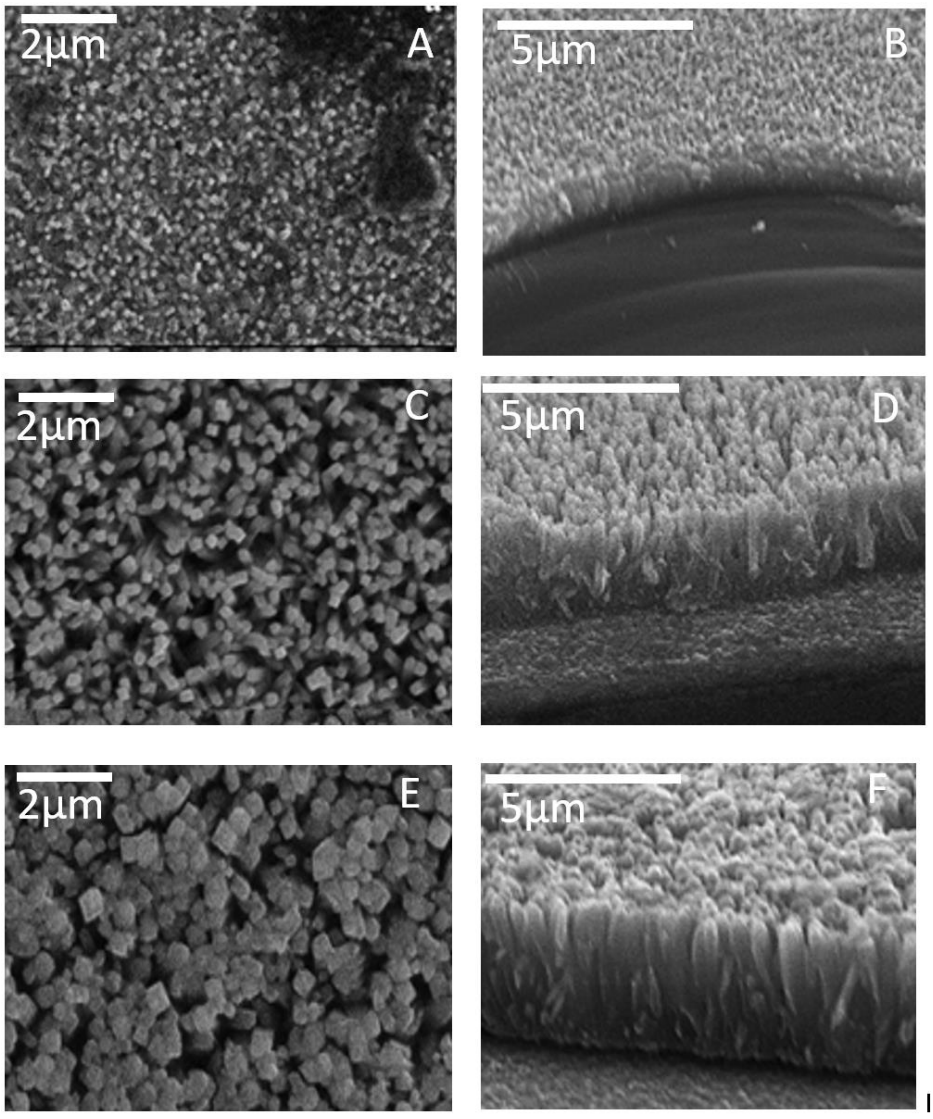

Figure 4. SEM images of Top and cross section view of TiO_2 nanorod grown at three different temperatures (A, B) 150 °C, (C, D) 160 °C, (E, F) 170 °C) for three hours of reaction duration.

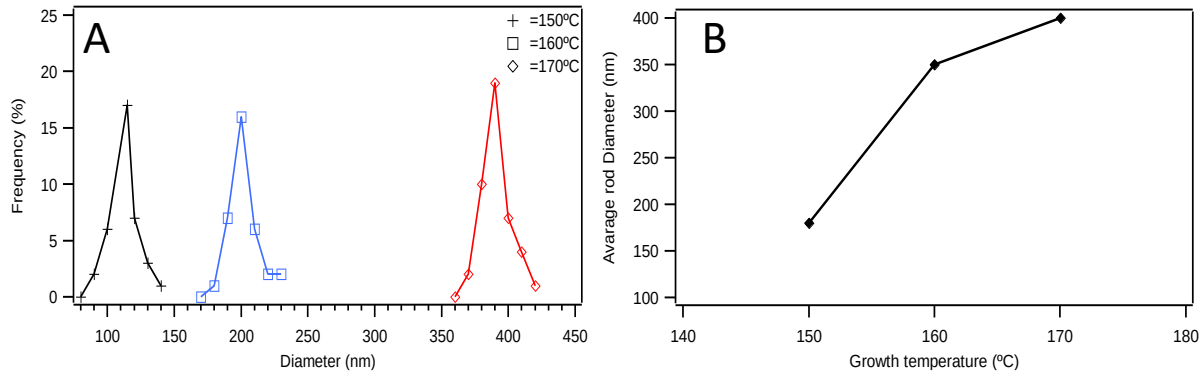

Figure 5. (A) Diameter distribution of TiO_2 nanorod arrays with varied growth temperature of 150°C, 160°C, and 170°C. (B): Average rod diameter as a function of growth temperature.

3.1.2 Effect of the Growth Temperature: The effect of hydrothermal temperature on the NR formation, the hydrothermal reaction time and initial TBO volume was kept constant at three hours and 0.3 ml respectively. Fig. 4 shows the effect of the growth temperature on the morphology of the nanorod. The rutile nanorods was grown at 150, 160 and 170 °C for three hours. The growth temperature was found to be an important factor affecting the morphology of the nanorods film as shown in the Fig. 4. An increase in the reaction temperature increases both diameter and length of the nanorods. However, the growth temperature has an influence on the diameter of the nanorods more than the length of the nanorods.

Figure5, shows the diameter distribution of the TNRs formed at different growth temperatures. It gives an indication that a strong relationship between the reaction temperature and the NRs diameter. Dropping the reaction temperature from 160 °C to 150 °C causes the TiO_2 film grew thin rods, the crystal domain size and FWHM with an average diameter of 115 nm to be 10.67 nm and 0.75º respectively. While the temperature is increased to 170°C the average nanorod diameter expands to 390 nm, and the crystal domain and FWHM are changed to 14.56 nm and 0.55º respectively, which indicate that the large difference in the size of the rods formed at high temperature, at higher temperature than 170 °C, the TNRs delaminated from the FTO substrate.

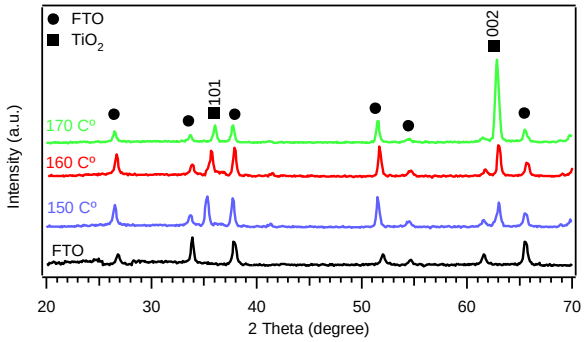

Figure 6. Shows XRD patterns of the rutile TiO_2 nanorod films on FTO substrates. These films were synthesised using three different reaction temperature and annealed at 550°C for three hours.

Figure 6 shows, X-ray diffraction (XRD) analysis of NRs that the two diffraction peaks at 36.3° and 63.2° correspond to the (101) and (002) planes of the tetragonal rutile TiO_2 crystal structure, respectively, NRs are single crystalline in tetragonal rutile structure. At 150°C the intensity ratio of (101) peak over (002) peak represents the degree of the alignment of the rutile nanorods, this indicates that the nanorods are more randomly oriented at the early stage of the growth. As the reaction time increases through 150°C to 170°C, the growth of the oblique nanorods is retarded and the well-aligned arrays of the vertical nanorods bury the oblique nanorods. Therefore, the relative intensity of (002) increases as the growth time increases and the intensity of (101) decreases.

3.1.3 Effect of Growth Tim: The initial titanium precursor volume and growth temperature were kept constant at 0.3ml and 160°C, respectively. Fig.7 (A-J), shows the top and cross-sectional SEM images of the single crystal TiO_2 NR arrays grown from 2-16 hours, the TiO_2 NRs is observed perpendicular to the surface and grows in a very high density over the entire FTO/glass substrates. At short duration of two hours in Fig.7 (A-B) low density of TiO_2 nanorods started growing on the FTO substrate about 140 ± 20 nm wide with not very uniform shape. With increased reaction time, NR orientation tends towards perpendicular to the surface; this observation was in good agreement with the XRD results.

The diameter distribution of the nanorod is plotted in Fig. 8 (a). It is noted that both width and length of the nanorods increase with reaction time, and the TNRs obtained after different reaction times have a mono- dispersed diameter. The nanorods after two hours of growth are about 1.3 µm in length and 140 nm in diameter with crystal domain size and FWHM 11.45 nm and 0.7º respectively. As the growth time is extended to three hours, average NR length and diameter are increased to about 2.2 µm and 190 nm in diameter. Growing the reaction time from three hours to five hours produces a load increase in rod diameter, from 190 nm to over 300 nm and length from 2.2 µm to 3.6 µm, with crystal domain size and FWHM to be 16.02 nm, 16.35 nm and 0.5º, 0.49º respectively. Therefore, decreasing of FWHM and increasing of the crystal size domain, indicating the formation of nanorods with a more varied diameter at a longer growth time. After 16 hours of growth very dense nanorods arrays were produced with 360 nm in diameter and length of 4.4 µm and the rods start to merge together and TiO_2 NRs delaminates from the FTO.

Figure 9, shows the change in the XRD patterns as a function of the growth time. All samples were annealed in air for three hours at 550 °C. This increases the crystallinity of the structure and also the adhesion of the TiO_2 film to the substrate. Relatively strong peaks can be respectively indexed to the (101) and (002). All the diffraction peaks are ascribed to tetragonal rutile phase. Phase TiO_2 corresponds to the peaks at 36.3° and 63.2° respectively. The strong peak (101) located at 36.3° indicates that the TiO_2 nanorods are crystalised well. The predominant (002) peak suggests that TiO_2 NRs grow with their c-axis orientation normal to the FTO surface and For long reaction times (16 hours), where the NRs are highly ordered perpendicular to the substrate surface, the (002) peak are dominant over (101). X-rays interact with the horizontal (002) plane of the roads, the result of this is a high intensity peak centered at 63.2°, as according to the SEM images. All the other peaks are related to the FTO substrate.

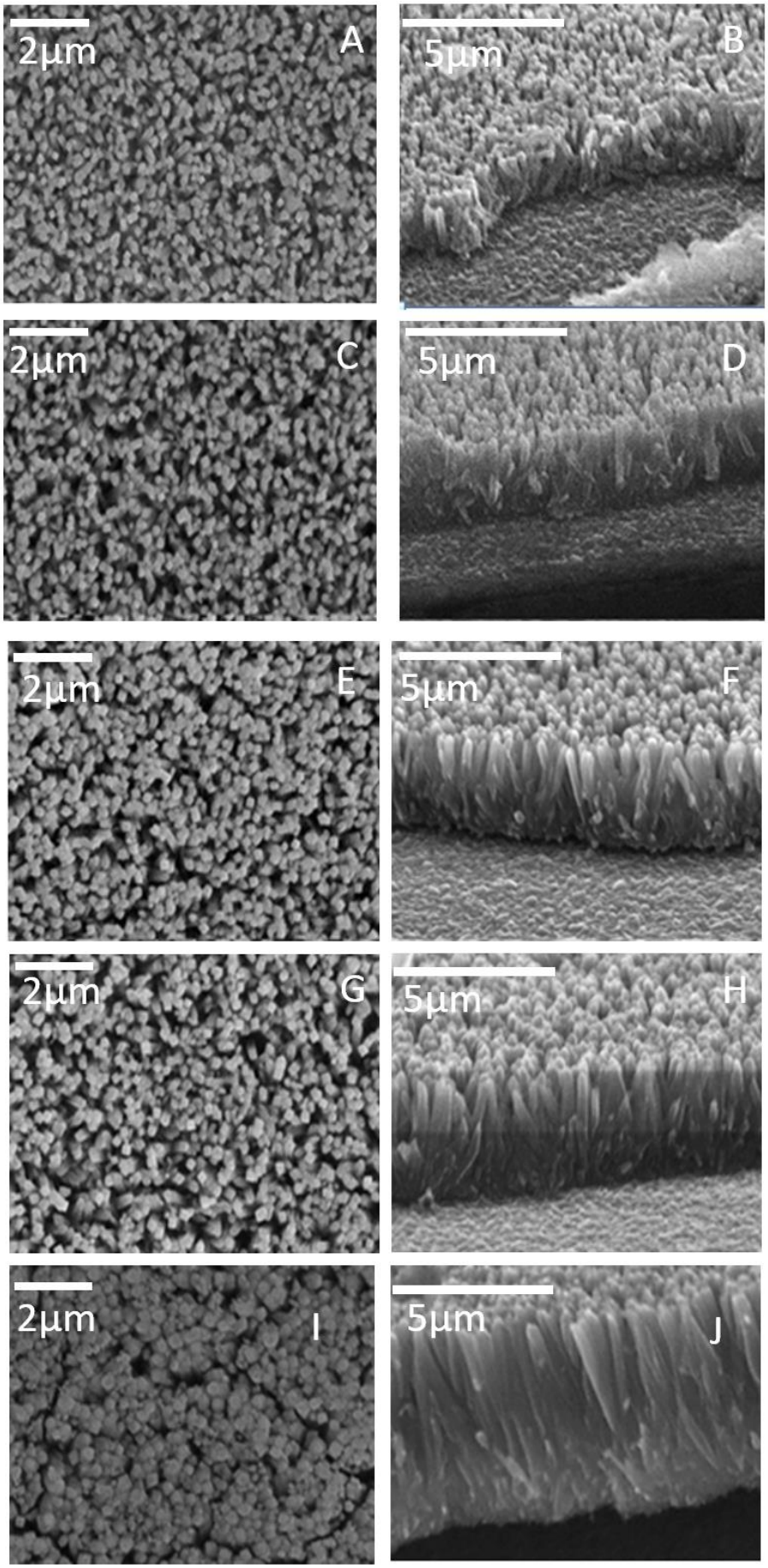

Figure 7. SEM image of TiO_2 nanorod at the different reaction time, Top and cross section view of: (A, B) 2 hours, (C, D) 3 hours, (E, F) 4 hours, (G, H) 5 hours, (I, J) 16 hours.

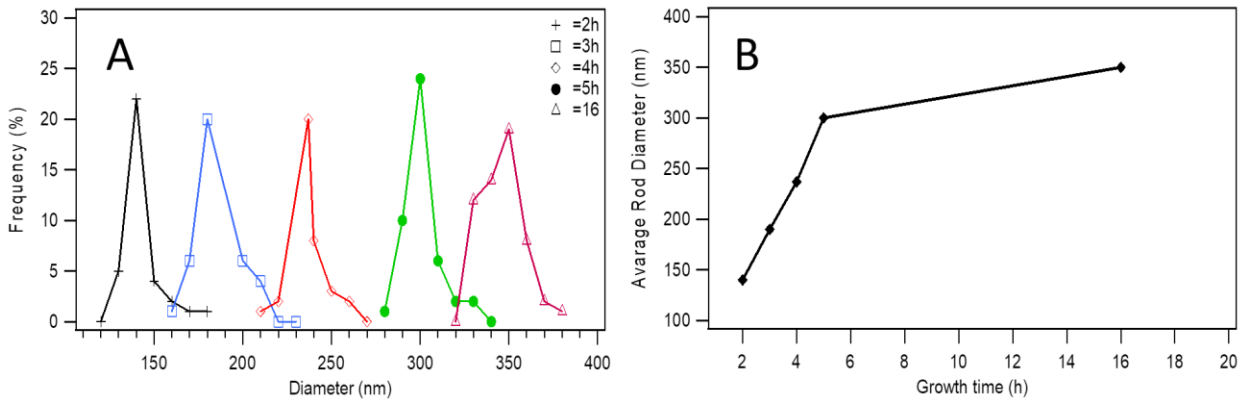

Figure 8. (A) Diameter distribution of TiO_2 nanorod arrays with different growth time of 2h, 3h, 4h, 5h and 16h. (B) Average rod diameter as function of growth time.

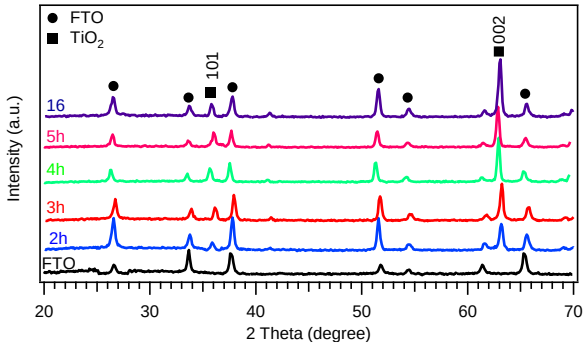

Figure 9. XRD patterns of TiO_2 nanorod arrays fabricated and annealed at 550°C for 3hours at the different reaction time: 2 hr, 3 hr, 4 hr, 5 hr, and 16 hr.

3.2 Effect of Hydrothermal Conditions on the PEC Water Splitting of TiO_2 Nanorod Films

Figure 10, shows the typical current density and photo conversion efficiency versus voltage curves of the TiO_2 nanorod arrays fabricated under different hydrothermal conditions, in PEC electrolyte of 1.0 M KOH (pH =13.2) exposed to 100 Mw cm^{-2} and the reversible oxygen standard potential is at 0.20 vs. Ag/AgCl. The dark current potential ranges from -0.5 V to 0.6 V.

The photoconversion efficiency percentage (η%) of the photoanode which converts the light energy into chemical energy is calculated via the following equation.(Fabrega et al., 2013; Li et al., 2011)

$$\eta(\%) = \left[\frac{(\text{total power output} - \text{electrical power input})}{\text{power density of incident light}}\right] \times 100 \qquad (2)$$

$$\eta(\%) = Jp[(E°rev - Eapp)]/I_0 \,] \times 100 \qquad (3)$$

Where, Jp= photocurrent density ($mAcm^{-2}$); J_p $E°rev$= total power output; J_p E_{app} = electrical power input; I° = power density of incident light ($mWcm^{-2}$). $E°_{rev}$ is the standard reversible potential which is 1.23 V vs. NHE, and E_{app}= potential between the working electrode and the counter electrode or the applied potential $E_{app} = E_{meas} - E_{oc}$, where E_{meas} is the electrode potential (vs. Ag/AgCl) of the working electrode at which photocurrent is measured under illumination. E_{oc} is the electrode potential (vs. Ag/AgCl) of the same working electrode at open circuit conditions under the same illumination and in the same electrolyte. The OCP is the potential difference between the working electrode (anode) and the reference electrode (Ag/AgCl) at equilibrium.

According to Fig. 10, the effect of the hydrothermal conditions on the PEC performance can be explained in the following points. Firstly, to examine the role of TBO concentration, the hydrothermal temperature and growth time were fixed at 150ºC and 3h as show in Fig. 10 (a and b), sample prepared using 0.3ml of TBO, nanorod array photo anode showed a photocurrent density as high as 1.8$mAcm^{-2}$ at 0.20 potential V vs. Ag/AgCl. And with a maximum photoconversion efficiency of ~1.4% was reached at - 0.12 V (vs. Ag/AgCl) was achieved by the sample prepared using 0.3ml of TBO. In contrast, samples prepared using 0.4ml and 0.5ml of TBO produce a photocurrent density of only 1.0 $mAcm^{-2}$ and 0.5 $mAcm^{-2}$ at 0.20 potential V vs. Ag/AgCl, respectively and photoconversion efficiency 0.6% and 0.3% at - 0.12 V (vs. Ag/AgCl) respectively.

Secondly, Fig.10(c and d), shows the photocurrent density and the photoconversion efficiency of the PEC mad with the as prepared TiO_2 electrode at different temperatures (150 ºC, 160 ºC and170 ºC) but TBO volume and growth time kept constant at 0.3 ml and three hours respectively, at short reaction temperature (150ºC) the sample generated a photocurrent density of 0.8 $mAcm^{-2}$ at 0.20 potential V vs. Ag/AgCl and exhibited a photo conversion efficiency of 0.5% at - 0.12V while increasing the temperature to (160ºC) more than double of photocurrent density (2.0 $mAcm^{-2}$) and photoconversion efficiency percentage(1.7%)was achieved, since they show the best PEC performance. Further increasing the reaction temperature to (170ºC) both photocurrent density and photoconversion efficiency starts to decrease because at this point the film to be thicker and the higher film thickness prevents UV light from penetrating through the nanorods film and therefore reduces the light absorption efficiency.

Finally, Fig. 10 (e-f), shows the photocurrent density and the photoconversion efficiency percentage of TiO_2 NR arrays grown from 2–16 h, after fixing the initial titanium concentration and the reaction temperature at 0.3ml and 160ºC. At a short reaction time (two hours) the sample produced a photocurrent density of 1.4 $mAcm^{-2}$ at 0.20 potential V vs. Ag/AgCl and showed a photo conversion efficiency of 1.0% at - 0.16V. Increasing the time to three hours showed the photocurrent increase to the extreme of 1.8 $mAcm^{-2}$ at 0.20 potential V vs. Ag/AgCl. This value was corresponds to the highest photo efficiency of 1.6% at -0.16 V. Further increasing the growth time to 16 hours induces both photocurrent density and photoconversion efficiency to 0.7 $mAcm^{-2}$ and 0.4% because the nanorod density and film thickness increase at high growth time, and the reasons will be discussed at the down.

Based on the data analysis, the photo electrochemical properties of the TNRs films are affected by two main factors: the nanorods density and the film thickness, both of which are directly influenced by the hydrothermal synthesis conditions. At low initial titanium concentrations, growth temperature and reaction time, nanorods arrays with low density, small diameter and low thickness are formed. The low nanorods density is important because it offers a high surface area to be in contact with the electrolyte. Moreover, low film thickness allows the illuminated

light to radiate through the whole nanorods layer. In contrast, wider nanorods diameter and density are obtained by increasing the growth conditions (concentration, temperature and time). In this case, a lower surface area nanorods film is used in the photocatalytic reaction. The higher film thickness prevents UV light from penetrating through the nanorods film and therefore reduces the light absorption efficiency. An aggregation at the base of the NRs formed at this stage of the reaction affects the charge separation and transportation, as it can act as charge recombination centre.

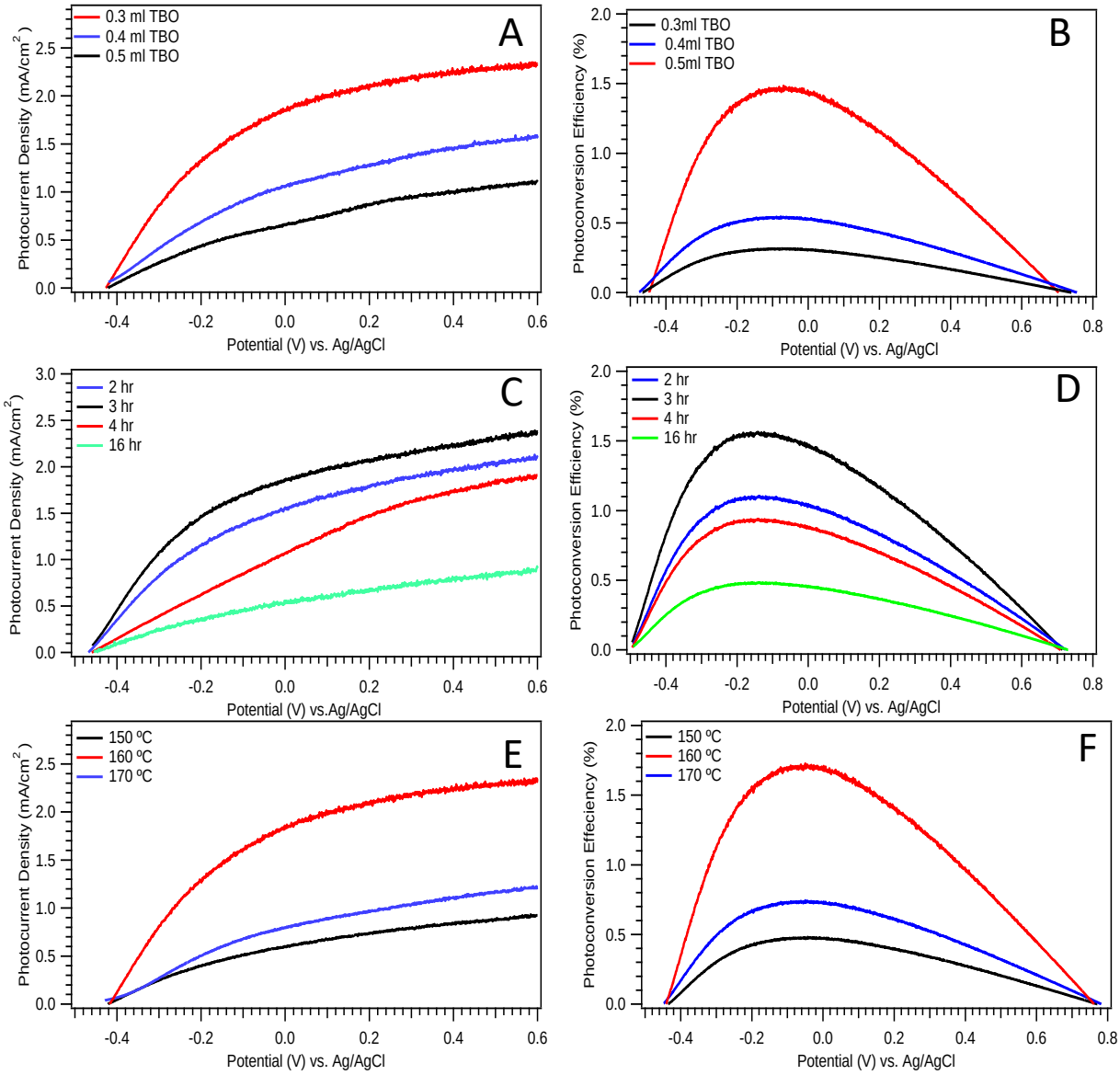

Figure 10. I-V curve of Photocurrent generated from TiO_2 NR films with the dark and under simulated AM 1.5 irradiation in 1.0 M KOH electrolyte (pH= 13.2) under the illumination of a 100 mW cm^{-2} solar simulator which were prepared under different hydrothermal conditions with calculated photo conversion efficiency. (a) And (b) show the effect of the initial titanium volume. (c) And (d) show the effect of the growth time. (e) And (f) show the effect of the growth temperature.

4. CONCLUSION

Highly oriented rutile TiO_2 nanorod arrays were prepared directly on the FTO substrates via a hydrothermal method, when used as photoanode to investigate their photoelectrochemical properties. The effect of hydrothermal conditions (precursor concentration, time and temperature) on morphology of the grown nanorod was investigated in detail. The nanorod arrays have been characterized using a scanning electron microscope (SEM), powder XRD and the Photoelectrochemical performance of the nanorod array photo anode was measured with a three-electrode cell. The results show that a low initial titanium concentration and short reaction time, with suitable growth temperature produce nanorod are generally well ordered, low density, and uniform in length and orientation with optimal photocatalytic performance. This is attributed to the low nanorods density, which offers a high surface area to react with the electrolyte, and short film thickness allows the incident UV light to penetrate through the entire film. Using 0.3ml of TBO C°, using a well-defined growth time (three hours) and temperature (160 °C) was found to be the ideal conditions to obtain optimised TNR films, with their associated superior PEC performance. This film yields a high photocurrent of 2.80 mA/cm^2, which corresponds to a photo conversion efficiency of 1.6%.

REFERENCES

Char, M. P., Niranjana, E., and Pai, K. V. (2008). Electrochemical studies of amaranth at surfactant modified carbon paste electrode: A cyclic voltammetry. *Int. J. Electrochem. Sci*, *3*(5), 588.

Dai, H. (2002). Carbon nanotubes: synthesis, integration, and properties. *Accounts of chemical research*, *35*(12), 1035-1044.

Fabrega, C., Andreu, T., and Morante, J. (2013). Optimization of surface charge transfer processes on rutile TiO_2 nanorods photoanodes for water splitting. *International Journal of Hydrogen Energy*, *38*(7), 2979-2985.

Feng, X., Shankar, K., and Grimes, C. A. (2008). Vertically aligned single crystal TiO2 nanowire arrays grown directly on transparent conducting oxide coated glass: synthesis details and applications. *Nano letters*, *8*(11), 3781-3786.

Fujishima, A. (1972). Electrochemical photolysis of water at a semiconductor electrode. *nature*, *238*, 37-38.

Fujishima, A., Rao, T. N., and Tryk, D. A. (2000). Titanium dioxide photocatalysis. *Journal of Photochemistry and Photobiology C: Photochemistry Reviews*, *1*(1), 1-21.

Guldin, S., Kohn, P., and Steiner, U. (2013). Self-cleaning antireflective optical coatings. *Nano letters*, *13*(11), 5329-5335.

Hashimoto, K., Irie, H., and Fujishima, A. (2005). TiO2 photocatalysis: a historical overview and future prospects. *Japanese journal of applied physics*, *44*(12R), 8269.

Hosono, E., Fujihara, S., and Imai, H. (2004). Growth of submicrometer-scale rectangular parallelepiped rutile TiO2 films in aqueous TiCl3 solutions under hydrothermal conditions. *Journal of the American Chemical Society*, *126*(25), 7790-7791.

Kazes, M., Lewis, D. Y., and Banin, U. (2002). Lasing from semiconductor quantum rods in a cylindrical microcavity. *Advanced Materials*, *14*(4), 317-321.

Kim, H., and Yang, B. L. (2015). Effect of seed layers on TiO 2 nanorod growth on FTO for solar hydrogen generation. *International Journal of Hydrogen Energy*, *40*(17), 5807-5814.

Kolen'ko, Y. V., Burukhin, A. A., and Oleynikov, N. N. (2003). Synthesis of nanocrystalline TiO 2 powders from aqueous TiOSO 4 solutions under hydrothermal conditions. *Materials Letters*, *57*(5), 1124-1129.

Lee, J. C., Kim, T. G., and Sung, Y. M. (2007). Enhanced photochemical response of TiO2/CdSe heterostructured nanowires. *Crystal Growth and Design*, *7*(12), 2588-2593.

Lee, J.C., Park, K.S., and Sung, Y.M. (2006). Controlled growth of high-quality TiO2 nanowires on sapphire and silica. *Nanotechnology*, *17*(17), 4317.

Lei, Y., and Wang, S. (2001). Preparation and photoluminescence of highly ordered TiO2 nanowire arrays. *Applied physics letters*, *78*(8), 1125-1127.

Li, Y., Yu, H., S and Shao, Z. (2011). A novel photoelectrochemical cell with self-organized TiO 2 nanotubes as photoanodes for hydrogen generation. *International Journal of Hydrogen Energy*, *36*(22), 14374-14380.

Lin, X., Song, D., and Qiang, Y. (2012). Synthesis of hollow spherical TiO 2 for dye-sensitized solar cells with enhanced performance. *Applied Surface Science*, *263*, 816-820.

Liu, B., and Aydil, E. S. (2009). Growth of oriented single-crystalline rutile TiO2 nanorods on transparent conducting substrates for dye-sensitized solar cells. *Journal of the American Chemical Society*, *131*(11), 3985-3990.

Liu, C., Tang, J., and Yang, P. (2013). A fully integrated nanosystem of semiconductor nanowires for direct solar water splitting. *Nano letters*, *13*(6), 2989-2992.

Lou, Z., Li, F., and Zhang, T. (2013). Branch-like hierarchical heterostructure (α-Fe2O3/TiO2): a novel sensing material for trimethylamine gas sensor. *ACS applied materials & interfaces*, *5*(23), 12310-12316.

Meng, N., Leung, M., and Leung, D. (2004). *Water electrolysis-a bridge between renewable resources and hydrogen.* Paper presented at the Proceedings of the international hydrogen energy forum.

Pan, Z. W., Dai, Z. R., and Wang, Z. L. (2001). Nanobelts of semiconducting oxides. *Science*, *291*(5510), 1947-1949.

Peng, X., Manna, L., and Alivisatos, A. P. (2000). Shape control of CdSe nanocrystals. *nature*, *404*(6773), 59-61.

Selman, A. M., and Hassan, Z. (2015). Structural and Photoluminescence Studies of Rutile TiO 2 Nanorods Prepared by CBD Method on Si Substrates. *American Journal of Materials Science*, *5*(3B), 16-20.

Shen, L., Bao, N., and Yanagisawa, K. (2008). Hydrothermal splitting of titanate fibers to single-crystalline TiO2 nanostructures with controllable crystalline phase, morphology, microstructure, and photocatalytic activity. *The Journal of Physical Chemistry C*, *112*(24), 8809-8818.

Sun, X., Sun, Q., and Dong, L. (2013). Significant effects of reaction temperature on morphology, crystallinity, and photoelectrical properties of rutile TiO2 nanorod array films. *Journal of Physics D: Applied Physics*, *46*(9), 095102.

Thamaphat, K., Limsuwan, P., and Ngotawornchai, B. (2008). Phase characterization of TiO2 powder by XRD and TEM. *Kasetsart J.(Nat. Sci.)*, *42*(5), 357-361.

Tsai, C. C., and Teng, H. (2006). Structural features of nanotubes synthesized from NaOH treatment on TiO2 with different post-treatments. *Chemistry of Materials*, *18*(2), 367-373.

Wang, Z. L., and Song, J. (2006). Piezoelectric nanogenerators based on zinc oxide nanowire arrays. *Science*, *312*(5771), 242-246.

Waterhouse, G. I., and Waterland, M. R. (2007). Opal and inverse opal photonic crystals: fabrication and characterization. *Polyhedron*, *26*(2), 356-368.

Wolcott, A., Smith, W. A., and Zhang, J. Z. (2009). Photoelectrochemical water splitting using dense and aligned TiO2 nanorod arrays. *Small*, *5*(1), 104-111.

Wu, M. C., Sápi, A., and Keiski, R. (2011). Enhanced photocatalytic activity of TiO2 nanofibers and their flexible composite films: Decomposition of organic dyes and efficient H2 generation from ethanol-water mixtures. *Nano Research*, *4*(4), 360-369.

Xie, Z., Zhang, Y., and Zhang, Z. (2013). Visible light photoelectrochemical properties of N-Doped TiO 2 nanorod arrays from TiN. *Journal of Nanomaterials*, *2013*, 9.

Zou, Y., Li, D., and Yang, D. (2012). Fabrication of TiO2 nanorod array/semiconductor nanocrystal hybrid structure for photovoltaic applications. *Solar Energy*, *86*(5), 1359-1365.

کورتیا لێکولینێ:

تۆێژالەك ژ TiO_2 nanorod یێ تاکە کریستال لسەر شیشێ (fluorine doped tin oxide (FTO) substrates) بڕێیا گەرمکرنا ب ئاڤێ هاتە ئامادەکرن. هەروەسا ئەڤ کارە گەلەك یێ بالکێشە ژبەر بکارهینانا وی یا باش د بیاڤێ شکاندنا گەردیلا ئاڤێدا. هەروەسا کارتێکرنا کاودانێن کارلێکێ لسەر مورفۆلۆجی , ئاراستێن کریستالا و چالاکیا هاندەر ب روناهیێ هاتە ئامادەکرن و هاتە پشکنینکرن و تیشکا ((X-ray diffraction (XRD) دیارکر کو دوو لوتکێن لادانێ ل 36.30 ,63.20 بەرامبەر تەختەیێ (101) ,(002) یا سیستەمێ چوارینەیی (rutile TiO_2 nanorod) لدوویڤ ئێك, هەروەسا نموونەیەك (عینە) ژ (SEM)دیارکر کو رووبەرێ ژدەرڤە , ئاراستێن وی و لگەل مورفولوجیێ پشتبەستنێ ب نەگوڕێن کارلێکێ دکەن وەك: پلاگەرمێ , دەمێ کارلێکێ و خەستیا .TiO_2 پشتی ئەڤ نەگوڕێن لسەری دیار هاتینە ڕێکخستن باشترین دوخ دیاربوو کو (0.3 ml ژ TBO و) 160(C0 بۆ ماوێ) 3 (h بچوویکترین نیڤ تیرە و درێژاهیا شەپولێ کو) 190 (nm, 2.2µmلدوویڤ ئێك. پشتی هاتیە ئامادەکرن دهاتە تیشکدان لژێر) 1.5 (Gتیشکێن روناهیێ کو هێزا وێ)100 (mWcm-2 بەرهەمهینا کو گرانیا تەوژمێ روناهیێ) 1.80 (mWcm-2 لگەل بلندترین و باشترین شیان بۆ گوهۆڕینا ب تیشکان 1.4% . هەروەسا ئەنجامان دیارکر کو چری و ڕێکوپێکیا TiO_2 nanorod گەلەك یاگونجایە بۆ بەرهەمهینانا H_2 ژ گردیلا H_2O ب سیستەمێ خانەیا کەهرو روناهیێ.